The Role of Chemokines in the Microenvironmental Control of T versus B Cell Arrest in Peyer's Patch High Endothelial Venules

By R.A. Warnock,*‡§ J.J. Campbell,*‡§ M.E. Dorf,‖ A. Matsuzawa,¶ L.M. McEvoy,** and E.C. Butcher*‡§

*From the *Laboratory of Immunology and Vascular Biology, Department of Pathology, and the ‡Digestive Disease Center, Department of Medicine, Stanford University Medical School, Stanford, California, 94305; the §Center for Molecular Biology and Medicine, Veterans Affairs Palo Alto Health Care System, Palo Alto, California 94304; the ‖Department of Pathology, Harvard Medical School, Boston, Massachusetts 02115; the ¶Institute of Medical Science, University of Tokyo, Tokyo 108-8639, Japan; and **DNAX Research Institute, Palo Alto, California 94304*

Abstract

Chemokines have been hypothesized to contribute to the selectivity of lymphocyte trafficking not only as chemoattractants, but also by triggering integrin-dependent sticking (arrest) of circulating lymphocytes at venular sites of extravasation. We show that T cells roll on most Peyer's patch high endothelial venules (PP-HEVs), but preferentially arrest in segments displaying high levels of luminal secondary lymphoid tissue chemokine (SLC) (6Ckine, Exodus-2, thymus-derived chemotactic agent 4 [TCA-4]). This arrest is selectively inhibited by functional deletion (desensitization) of CC chemokine receptor 7 (CCR7), the receptor for SLC and for macrophage inflammatory protein (MIP)-3β (EBV-induced molecule 1 ligand chemokine [ELC]), and does not occur in mutant DDD/1 mice that are deficient in these CCR7 ligands. In contrast, pertussis toxin–sensitive B cell sticking does not require SLC or MIP-3β signaling, and occurs efficiently in $SLC^{low/-}$ HEV segments in wild-type mice, and in the SLC-negative HEVs of DDD/1 mice. Remarkably, sites of T and B cell firm adhesion are segregated in PPs, with HEVs supporting B cell accumulation concentrated in or near follicles, the target domain of most B cells entering PPs, whereas T cells preferentially accumulate in interfollicular HEVs. Our findings reveal a fundamental difference in signaling requirements for PP-HEV recognition by T and B cells, and describe an unexpected level of specialization of HEVs that may allow differential, segmental control of lymphocyte subset recruitment into functionally distinct lymphoid microenvironments in vivo.

Key words: receptors, lymphocyte homing • receptors, chemokine • cell adhesion • endothelium, vascular • lymphoid tissue

Introduction

Recirculating naive lymphocytes are recruited from the blood stream into the secondary lymphoid tissues of Peyer's patches (PPs)[1] and LNs via selective interactions with high endothelial venules (HEVs). Lymphocyte recognition of HEVs involves a multistep adhesion cascade in which primary adhesive interactions (rolling) are followed by firm arrest (sticking) in response to pertussis toxin (PTX)-sensitive rapid signaling events (1–3; for a review, see reference 4). Although the functional contribution of endothelial and lymphocytic adhesion molecules has been characterized (1–5), the identity and physiological roles of the signaling receptor(s) and their ligand(s) involved in lymphocyte–HEV recognition have not been defined.

Recent evidence has highlighted the potential role in lymphocyte migration and homing of a relatively new class of soluble leukocyte chemoattractants called chemokines, which signal through PTX-sensitive $G_{\alpha i}$-linked serpentine receptors (6, 7). PPs and peripheral LNs (PLNs) express

Address correspondence to Eugene C. Butcher, Department of Pathology L-235, Stanford, CA 94305. Phone: 650-493-5000 ext. 63130; Fax: 650-858-3986; E-mail: ebutcher@stanford.edu

[1]*Abbreviations used in this paper:* CCR, CC chemokine receptor; CMFDA, carboxymethylfluorescein diacetate; cRPMI, RPMI 1640 supplemented with 10% bovine calf serum and 10 mM Hepes; CXCR, CXC chemokine receptor; DNP, dinitrophenol; HEV, high endothelial venule; LM, labeling medium; LNC, LN lymphocyte; MAdCAM, mucosal addressin cell adhesion molecule; MIP, macrophage inflammatory protein; MLN, mesenteric LN; PLN, peripheral LN; PP, Peyer's patch; PTX, pertussis toxin; SDF, stromal cell–derived factor; SLC, secondary lymphoid tissue chemokine.

message RNA for at least three chemokines, including secondary lymphoid tissue chemokine (SLC) and macrophage inflammatory protein (MIP)-3β, which act through a common CC chemokine receptor, CCR7; and stromal cell–derived factor (SDF)-1α, which signals through CXC chemokine receptor (CXCR)4; each of which attracts the majority of lymphocytes (8–11), including the naive cells that characteristically home to secondary lymphoid organs (12). We and others have hypothesized that CCR7 on lymphocytes may be critical for lymphocyte–HEV interactions because CCR7 ligands are most abundant in secondary lymphoid tissues and, in particular, because SLC message is expressed by endothelial cells of HEVs (10). Furthermore, recent in vitro studies have demonstrated rapid adhesion and transendothelial chemotaxis of B and T cells in response to CCR7 ligands in assays that model in vivo shear and adhesive environments of secondary lymphoid tissues (8, 10, 14, 15). To explore the involvement of CCR7 and its ligands in physiological lymphocyte interactions with PP-HEVs, we selectively attenuated CCR7 function in lymphocytes by ligand desensitization, observed their interactions in situ using intravital microscopy, and compared their behavior with that of normal lymphocytes interacting with SLC-deficient HEVs in DDD/1 mice. In addition, we assessed the in situ display of CCR7 ligand SLC by PP-HEVs using confocal microscopy, compared SLC localization with sites of lymphocyte accumulation, and investigated the differential accumulation of T and B cells in PP-HEVs.

Our results demonstrate that SLC is displayed by a subset of HEVs that support T cell arrest, and that absence of SLC presentation by HEVs or functional inhibition of the SLC/MIP-3β receptor CCR7 abrogates the firm arrest of T but not B cells in PP-HEVs. Together, these data suggest a critical role for CCR7 in T cell–HEV recognition, and reveal a fundamental difference in the signaling requirements for T and B cell recruitment to PP-HEVs. Furthermore, our studies demonstrate an unexpected segregation of HEV sites of T and B cell accumulation within PPs, correlating with differential chemokine display in well-defined microenvironmental domains. These results suggest a novel mechanism for the microenvironmental targeting of lymphocyte subsets, at the level of HEV recognition and recruitment from the blood.

Materials and Methods

Reagents. CellTracker™ Green, 5-chloromethylfluorescein diacetate (CMFDA; Molecular Probes, Inc.) was prepared as a 0.5 mg/ml stock solution in DMSO, stored at −30°C, and used within 1 wk. Tetramethylrhodamine-5-(and-6)-isothiocyanate (5[6]-TRITC; Molecular Probes, Inc.) was prepared as a 2 mM solution in DMSO, diluted to a stock 1:10 with saline, sterile filtered, and stored in single aliquots at −30°C. Alexa™ 488 and Alexa™ 546 protein labeling kits were used as directed by the manufacturer (Molecular Probes, Inc.). Chemokines mouse SLC (Exodus-2/thymus-derived chemotactic agent 4 [TCA-4]/6Ckine; a gift of DNAX Research Institute), human MIP-3β (ELC), and human SDF-1α (PeproTech) were prepared as 0.5 mg/ml stock solutions in saline and used immediately, or stored as aliquots at −80°C. Labeling medium (LM) was 50% RPMI 1640 and 50% Ca/Mg-free HBSS (BioWhittaker), supplemented with 1.5% bovine calf serum and 10 mM Hepes (cRPMI) (Sigma Chemical Co.) and was made fresh daily.

mAbs. mAbs Mel-14 (rat IgG2a, anti–mouse L-selectin [16]), MECA 79 (rat IgM, anti–peripheral node addressin [PNAd]), MECA 367 and MECA 89 (rat IgM, anti–mucosal addressin cell adhesion molecule [MAdCAM]-1 [17]), 9B5 (rat IgM, anti–human CD44), and 4B1E7C10 (hamster IgG, anti–mouse SLC [18]) were generated in our laboratories. Hybridoma cells for these mAbs as well as mAbs UC8-1B9 (hamster IgG, anti-dinitrophenol [DNP]; American Type Culture Collection), Tib 213 (rat IgG2b, anti–mouse CD11a; American Type Culture Collection [19]), and PS/2 (rat IgG2b, anti–mouse CD49d; American Type Culture Collection) were purified from culture supernatant. mAbs were stored at −80°C in endotoxin-free saline at 1 mg/ml. For in situ staining studies, 12–75 μg of antibody was injected via left carotid arterial cannulation. FITC-, Alexa™ 488–, and Alexa™ 546–conjugated mAbs to DNP, human CD44, mouse L-selectin, mouse CD11a, mouse CD49d, mouse SLC, and mouse MAdCAM-1 were made in our laboratories. FITC-conjugated mAbs to murine CD3 and B220 were from PharMingen.

Lymphocyte Isolation and Treatment. LN cells (LNCs) were freshly isolated from PLNs (axillary, brachial, cervical, and subiliac) and mesenteric LNs (MLNs). Splenocytes were freshly isolated from disaggregated spleens, and cleared of red blood cells using a Whole Blood Erythrocyte Lysing kit (R&D Systems). Cells were incubated for 1 h at 37°C in cRPMI, then washed and resuspended to 1.5×10^7 cells/ml in warm LM. Representative samples were stained with FITC-conjugated mAbs to T and B cell markers (CD3 and B220, respectively) and determined by flow cytometry to be ~95% lymphocytes. For isolation of T and B cell populations, negative selection columns were used as directed by the manufacturer (R&D Systems, and Cedarlane). Purity as determined by CD3 or B220 staining was on average >96% for T cells, and >90% for B cells. For fluorescent labeling, 2 ml LNCs was incubated with 4 μM CMFDA or 0.8 μM TRITC in LM for 10 min at 37°C. Lymphocytes were centrifuged through 2 ml of warm bovine calf serum, and supernatant was discarded. The pellet was resuspended to 1.5×10^7 cells/ml in warm LM. Aliquots of LNCs were treated with chemokine or saline for 45 min, washed again through serum, resuspended at 1×10^8 cells/ml in warm saline, and used immediately.

Animals. We used adult BALB/c and DDD/1 (23) mice (bred in the animal facility of Palo Alto Veterans Medical Center) of both sexes (10–14 wk, 18–25 g body wt) as recipients for in vivo experiments, and young BALB/c mice (6–10 wk, 12–20 g body wt) as lymphocyte donors. All experimental procedures comply with National Institutes of Health guidelines for the care and use of laboratory animals, and were approved by the Standing Committees on Animals of Stanford Medical School and The Palo Alto Veterans Medical Center. Animals were under complete surgical anesthesia throughout all experimental procedures.

PP Preparation and Intravital Microscopy. Mice were anesthetized by intraperitoneal injection (10 ml/kg) of physiologic saline containing xylazine (1 mg/ml) and ketamine (5 mg/ml). A loop of small intestine displaying at least one PP was prepared for intravital microscopy as described previously (1, 2) with modifications. In brief, a polyethylene catheter was inserted in the left carotid artery and was used for injection of cell suspensions and mAbs. A midline incision was made to expose the peritoneal cavity, and a jejunal or duodenal loop was exposed and arranged

within a rubber O-ring upon a small raised platform attached to a stage, and kept moist with warm saline. After the PP to be examined was positioned, a glass coverslip was applied to enclose the preparation for microscopic viewing. The stage was then placed on a Nikon intravital microscope equipped with a silicon-intensified target camera (Cohu, Inc.). The PP was visualized by epifluorescence from a mercury lamp source. Video images were recorded using a time-base generator (For-A) and a VHS VCR (JVC). Venular segments to be video-recorded were located by the characteristic autofluorescence of stromal elements in PP primary follicles, and identified by characteristic physical structure.

Analysis of In Situ Lymphocyte Behavior in PP-HEVs. Boluses (100–200 μl) of fluorescently labeled LNCs or splenocytes (10^8 cells/ml) were retrogradely injected via the carotid artery catheter over 30 s. Lymphocyte behavior in PLNs was recorded through 16× Neofluor (Nikon) or 20× water immersion objective (Achroplan; Carl Zeiss, Inc.). Cell behavior in individual vessel segments was determined by playback of videotapes. For each experiment, cells of one color were selected as the experimental population, and these cells were resuspended after fluorescent labeling to 1.5×10^7/ml, aliquoted into two tubes, and incubated with chemokine (desensitized test cells) or control medium (mock-treated control cells) for 45 min at 37°C, then washed by centrifugation through a serum cushion. Cells of the other color, used as an internal standard population, were similarly washed after labeling, then mixed at ~1:1 ratio with the experimental test or control cells at a final concentration of 10^8 cells/ml in warm saline. (Aliquots of injected mixtures were saved for FACS® analyses to determine the precise ratio of experimental to standard cells injected.) Cells were then immediately injected via carotid artery cannula into mice prepared for intravital microscopy. Areas within the selected PPs were surveyed in the initial 2 min for HEVs supporting lymphocyte interactions, and then observed for an additional 10 min. Microscope filter sets were alternated every 30 s to allow observations of differently labeled (experimental versus internal standard) cells, thus allowing comparison of behavior of identically labeled test (chemokine-treated) cells versus mock-treated (control) cells, in littermate animals, with the behavior of the same internal standard cell population.

The total number of cells entering HEVs in the blood per minute was defined as the total cell flux. Cells were considered noninteracting when they moved at the velocity of RBCs, appearing as streaks on videotape images. These were easily distinguished from rolling cells, whose velocity is typically 10-fold lower: these rolling cells appear as circles on each video frame, and were characterized by velocities in our experiments <300 μm/s (generally 20–150 μm/s, similar to previous reports [2, 3, 43]). Cells were considered interacting whether they rolled, arrested, or both. The rolling fraction is the percentage of cells that interact with a given venule in the total number of cells that enter that venule during the same period. Velocities of >15 consecutive rolling lymphocytes were calculated as described (1). Sticking/arrest or firm adherence was defined as interacting cells that become immobile for >3 s (1). Total flux and rolling fraction data were collected during a period 4–8 min after injection, and represent at least 10 consecutive cells in at least 10 HEVs per preparation. Accumulated cells (i.e., cells that did not move during a 30-s observation) in the same HEV were enumerated at the 8-min time point. The values of total flux, rolling fraction, or accumulated cell numbers for the experimental population were normalized to those of the coinjected internal standard cells assessed within the HEV and time period, thus controlling for natural variability in hemodynamics and vascular characteristics. The resulting ratio provides an index of the behavior of the chemokine-treated test cells (e.g., the total flux of test cells divided by the flux of internal standard cells), and this index is then expressed as a percentage of that of the index of control (mock-treated) experimental cell flux/internal standard cell flux determined in parallel littermate animals. The control experiments using the mock-treated cells were performed immediately before and after those using chemokine treatments. The use of internal standard populations, and the analysis of data and results of in vivo homing data in this manner have been discussed in more detail elsewhere (12).

Statistical Methods. Data in graphs are shown as means ± SD, unless otherwise indicated. For statistical comparison of two samples, a two-tailed Student's *t* test was used when applicable. Differences were considered statistically significant when $P < 0.05$.

Results

Chemokine-desensitized Lymphocyte Interactions in PP-HEVs. Lymphocytes exposed to high concentrations of a chemokine become refractory to subsequent stimulation with the same chemokine, or other agonists that signal through the same receptor(s). This selective unresponsiveness is thought to be mediated by the well-described phenomenon of ligand-induced homologous receptor desensitization (20, 21). We have previously shown that SLC and MIP-3β can desensitize mouse LNCs, as well as human PBLs, and that these chemokines signal via the same chemokine receptor, CCR7 (22). Here we asked whether desensitization of lymphocytes with SLC, which is expressed by HEVs and can trigger rapid integrin-mediated adhesion in vitro, could inhibit in situ signals that trigger integrin-mediated firm adhesion of rolling lymphocytes. We observed the behavior of chemokine-treated or control lymphocytes within PP-HEVs, while recording video images for later analysis. Unfractionated, monocyte-depleted LNCs derived from PLNs and MLNs were fluorescently labeled, then pretreated with chemokine or control media before use. Cells were washed through a warm serum gradient and immediately injected into a mouse prepared for intravital microscopy.

Desensitization with CCR7 ligand SLC, but not with the CXCR4 ligand SDF-1α, substantially inhibits accumulation of intravenously injected LNCs in PP-HEVs in vivo (Fig. 1). Total flux and rolling fraction of SLC-treated lymphocytes through HEV were, if anything, slightly increased over control. Rolling velocity (Fig. 1 legend) and surface levels of adhesion receptors L-selectin, LFA-1, and α4β7 on desensitized lymphocytes (data not shown) remained unchanged from mock-treated control. Chemokine desensitization dramatically reduced the conversion of rolling to sticking behavior and firm arrest, an effect that is similar to PTX treatment and consistent with inhibition of the specific $G_{\alpha i}$ protein–linked signaling event required for integrin-mediated activated rapid adhesion.

Distinct Requirements for Activation-dependent Arrest of T versus B Lymphocytes. The incomplete inhibition of LNC accumulation by SLC desensitization led us to ask if there was a subset of lymphocytes that could adhere independently of CCR7 signaling. We found that SLC or MIP-3β

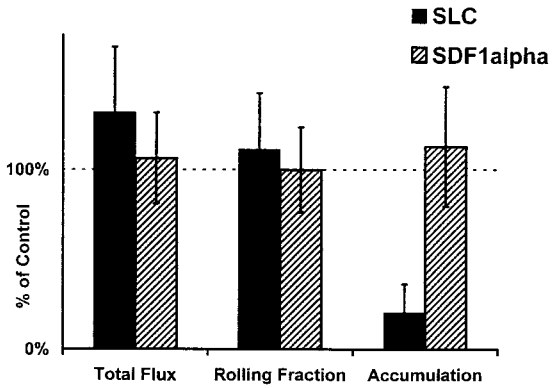

Figure 1. Desensitization of LNCs with SLC inhibits arrest in PP-HEVs. Unfractionated LNCs (70–85% $CD3^+$ by FACS®) of young mice were washed and incubated in cRPMI for 1 h in tissue culture flasks. LNCs were fluorescently labeled, incubated with chemokine (SLC and SDF-1α) or control medium for 45 min at 37°C, washed through a warm serum gradient to remove residual chemokine, and resuspended together with internal standard cells (labeled in a different color) immediately before injection via carotid artery cannulation into mice prepared for intravital microscopy. Areas within the visualized PPs were surveyed in the initial 2 min for HEVs supporting lymphocyte interactions, and then observed for a further 10 min. Total flux and rolling data (for test and for internal standard cells) were collected during a 2-min period 6–8 min after injection, and represent at least 10 consecutive cells of each type in at least 10 HEVs per preparation. Accumulated cells in these same HEVs were enumerated at the 8-min time point. Lymphocyte total flux, rolling fraction, or accumulation was variable in different vessels and PPs, reflecting the natural variability in hemodynamic parameters and vascular characteristics. Therefore, values determined for experimental cells (chemokine-desensitized or mock-treated cells of one color) were normalized by dividing by values obtained for coinjected internal standard population (labeled in a separate color) determined in the same recipient vessels. The ratio of chemokine-treated cell to internal standard cell values (e.g., rolling fractions), determined in one set of recipients, was then divided by the ratio of mock-treated control cell to internal standard cell values determined in littermate recipients, and multiplied by 100. Thus, the data presented represent the total flux, rolling fraction, or accumulation of chemokine-treated cells expressed as a percentage of those of mock-treated control cells labeled identically and analyzed in parallel. Therefore, 100% in the graph represents the behavior of the mock-treated control cells: for these cells, the total flux of cells entering HEVs in the blood per minute ranged from 16 to 60, mean 36 ± 14 SD in a representative experiment; the rolling fraction ranged from 27 to 100%, mean 69 ± 20% SD; and the number of cells accumulated in HEV segments ranged from 0 to 60 or more by 10 min. These values illustrate the natural variability associated with different vascular segments and observation periods that necessitated the use of internal standard cells for these studies. Rolling velocity ranged from 25 to 170 μm/s, mean 81 ± 46 SD. Mean results of five experimental animals for each treatment (± SD) are shown in the graph. Inhibition of accumulation by SLC treatment is significant compared with SDF-1α or control treatment by Student's *t* test ($P < 0.01$).

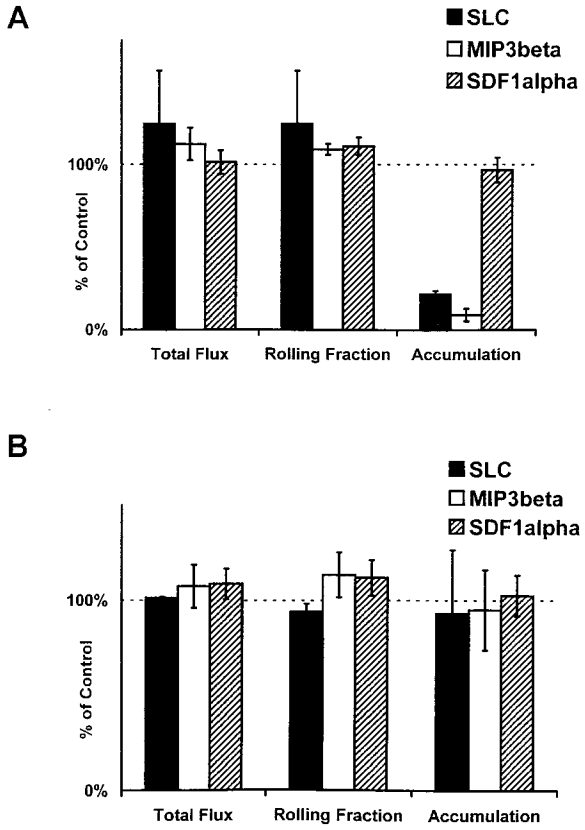

Figure 2. Effect of chemokine desensitization on T and B cell interactions with PP-HEVs. (A) T cell or (B) B cell subpopulations of LNCs were enriched by negative selection (see Materials and Methods), labeled, and incubated with 1 μM of indicated chemokine or control medium as in Fig. 1, then injected (mixed 1:1 with internal standard cells), and their behaviors were observed within PP-HEVs. Data collection was as in the legend to Fig. 1 except for B cells (which accumulated faster than T cells; data not shown), for which total flux and rolling fraction were analyzed during a 2-min time period 4–6 min after injection. Data are percentages of mock-treated control, and represent mean results of two to four experimental animals for each combination of subset and treatment (± SD). Control T cell total flux in vessels examined ranged from 14 to 60 cells/min, mean 48 ± 24 SD, and rolling fraction from ~35 to 93%. Control B cell total flux ranged from 8 to 74 cells/min, mean 32 ± 18 SD, and rolling fraction from 25 to 84%, mean 54 ± 23%. Rolling velocity of T cells (range 23–197 μm/s, mean 94 ± 33 SD, comparable to previous reports [references 2, 41]) was not effected by SLC desensitization (range 24–160 μm/s, mean 99 ± 44 SD). B cell rolling velocities were similar (range 27–120 μm/s, mean 55 ± 25 SD). Inhibition of T cell accumulation by SLC or MIP-3β desensitization is significant compared with control or SDF-1α desensitization by Student's *t* test ($P < 0.01$).

pretreatments dramatically attenuated T cell accumulation, acting, as above, at the level of triggered firm arrest (Fig. 2 A). Total flux, rolling fraction (Fig. 2 A), and rolling velocity (see Fig. 2 legend) for treated T cells were indistinguishable from control. Although these results do not formally exclude an effect of SLC or MIP-3β pretreatment on signaling through other adhesion-triggering receptors, they are consistent with a requirement for CCR7-dependent T cell recognition of HEVs. In contrast, preincubation with CCR7 ligands had no effect on B cell behaviors in PP-HEVs (including accumulation, Fig. 2 b), even though this treatment effectively inhibited the robust chemotactic response of B cells to homologously signaling agonists in vitro (Fig. 3). Importantly, B cell accumulation was inhibited by PTX treatment, confirming the involvement of a $G_{\alpha i}$ heterotrimeric G protein–mediated signaling event (data not shown). Together, these results suggest that B cell firm arrest in HEVs is triggered by a chemokine (or other chemoattractant) receptor independent of or in addition to CCR7.

To evaluate further the apparent difference in T versus B cell requirement for CCR7 signaling, we took advantage

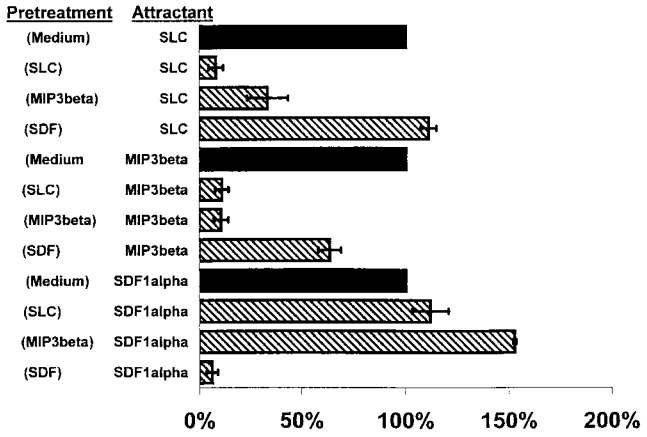

Figure 3. Homologous but not heterologous desensitization by CCR7 and CXCR4 ligands. Desensitization of chemotaxis experiments were performed as described (reference 22). In brief, mouse LN or spleen cells were pretreated with five times the optimal chemotactic dose of the indicated chemokine (or control medium), and washed through a serum layer to remove residual chemokine. The desensitized cells were then allowed to migrate towards the same or another chemokine (at the optimal chemotactic dose) through 5-μm pores for 15 min. Migrated cells were counted as described (references 8, 22). Percent migration of B cells was calculated based on FACS® analysis of migrated compared with input cells; B cells were defined as $CD3^-/CD19^+$. Data shown are the mean ± SD of three experiments, each with two replicate wells per condition. Mean maximum migration of mock-treated control B cells to SDF-1α was 10%, to MIP-3β 15%, and to SLC 13%.

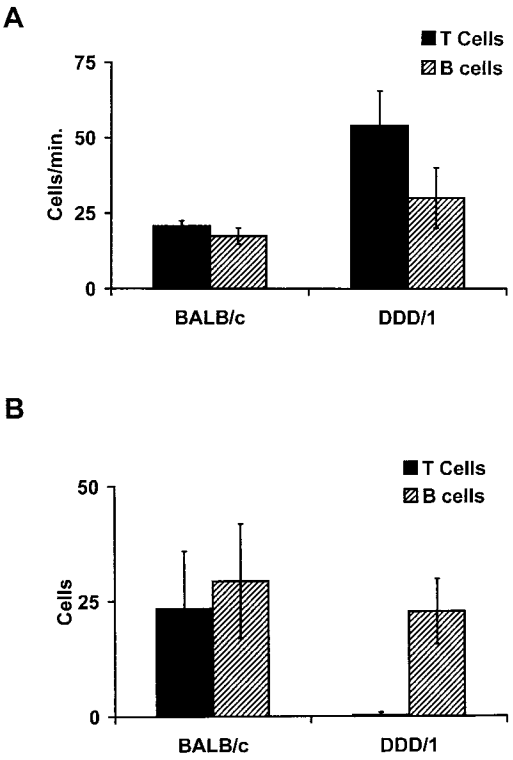

Figure 4. Interactions of T and B cells with PP-HEVs of DDD/1 versus normal mice. (A) The rolling flux of injected T cells (black bars) in PP-HEVs is increased in SLC-deficient DDD/1 mice compared with age-matched normal BALB/c, while B cell (hatched bars) rolling flux is comparable. (B) T cell accumulation is severely curtailed in PP-HEVs of DDD/1 mice; B cell accumulation is similar to control BALB/c mice. Enriched T and B cell (10^7 cells each) populations were differentially labeled and coinjected for observation in PP-HEVs. Venular trees draining single follicles were selected for analysis. Rolling flux is the total number of rolling B or T cells observed over time and averaged for the number of venules that supported rolling in the tree. Accumulation is the average number of stuck cells of each subset in the whole tree at 8 min after injection. Data are mean results of three experimental animals of each type (± SD). Rolling velocities of T cells in DDD/1 mice were similar to those in wild-type BALB/c mice (range 43–191 μm/s, mean 99 ± 44 SD).

of the DDD/1 mouse strain. DDD/1 mice have greatly reduced numbers of T cells in LNs and PPs, but have almost normal B cell numbers. Short-term homing assays suggest abnormalities in T cell migration into lymphoid tissues, although adhesive interactions between lymphocytes and HEVs in Stamper-Woodruff frozen section assays were normal (23, 24). The mice have a genetic defect in one of two SLC genes (the one expressed in lymph nodes; see Note added in proof). Lymphoid tissues of DDD/1 mice lack mRNA for SLC, and MIP-3β transcription is severely reduced as well (24). We reasoned that the defect in T cell lymphocyte homing in DDD/1 mice could be due either to a deficiency in T cell interactions with HEVs in situ, or else to an absence of directed migration of HEV-bound cells into LNs as had been speculated previously (23, 24). To distinguish between these possibilities, we compared the in situ behavior of enriched wild-type T and B lymphocyte populations interacting with PP-HEVs of DDD/1 mice with their interactions in normal mice. While B cell interactions were similar in recipients of the two genotypes, there was a striking lack of T cell arrest in DDD/1 PPs (Fig. 4). The T cell rolling flux in DDD/1 mice was significantly higher than in normal mice within 6 min, presumably due to the inability of naive T cells to localize in mutant organized lymphoid tissues. Thus, lymphocyte behavior in DDD/1 PP-HEVs is equivalent to that of specific SLC- and MIP-3β–desensitized T and B cells in normal mice (Fig. 2).

Our data suggest that CCR7 but not CXCR4 is critically involved in the triggering of T cell rapid adhesion in PP-HEVs. In contrast, triggered adhesion and firm arrest of B cells involve distinct mechanisms independent of (or in addition to) SLC, MIP-3β, and SDF-1α, and their receptors.

Microenvironmental Control of Lymphocyte Recruitment. We wished to address further the role of SLC, speculating that for SLC to trigger adhesion of blood-borne lymphocytes, it must be presented on the lumen of HEVs. We intravenously injected fluorescently labeled anti–mouse SLC mAbs, anti–MAdCAM-1 mAbs, or control mAbs into normal BALB/c mice for intravital staining of vessel endothelium (Fig. 5). Anti-SLC reacted with most $MAdCAM\text{-}1^+$ HEVs in PPs, but reactivity was variable in different regions. The most intensely staining segments were predominately located within interfollicular areas, whereas $MAdCAM\text{-}1^+$ HEVs lacking detectable SLC were most common in or adjacent to follicles. Presentation of SLC by segments of venular trees draining individual follicles was also variable, particularly in

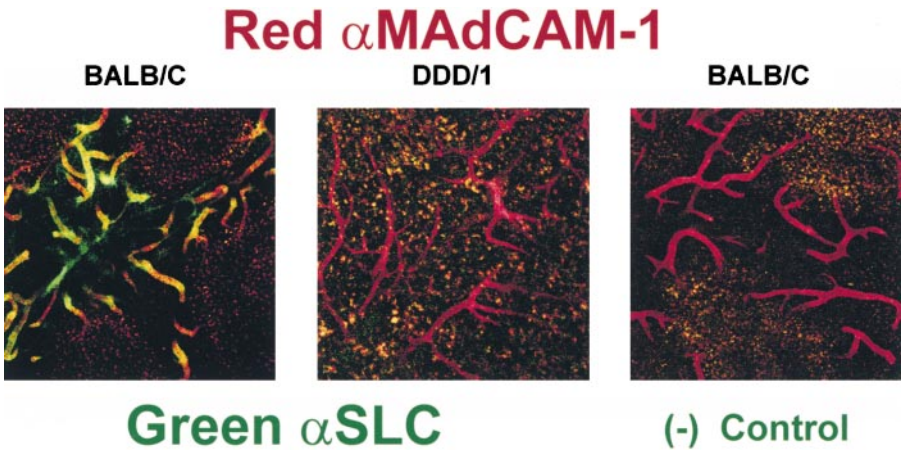

Figure 5. SLC is expressed on the lumen of PP-HEVs in normal, but not DDD/1 mice. Confocal micrographs of whole PPs from normal (left and right panels) or DDD/1 (middle panel) mice depicting localization of green anti-SLC (left and middle panels), and lack of green staining with a negative control hamster antibody (right panel); and MAdCAM-1$^+$ HEVs as red fluorescence (all three panels). mAbs to SLC (anti–TCA-4, 4B1E7C10 [reference 17]) and MAdCAM-1 (MECA 89), or control antibodies to DNP (UC8-19B) and human CD44 (Hermes-1) (not shown) were conjugated to Alexa™ 488 or Alexa™ 546, respectively. 50–75 μg of anti-SLC or anti-DNP, and/or 10–20 μg anti–MAdCAM-1 or anti-huCD44 was injected via carotid artery cannulation in a single bolus. Staining was evident for both SLC and MAdCAM-1 by 1 min, maximal for MAdCAM-1 by 10 min and for SLC by 15 min. Animals were killed, and whole PPs were immediately removed for examination by confocal microscopy. Representative images (10× objective).

older mice. Anti-SLC reactivity appeared stronger in PPs of young mice, and rarely, a small section of a precapillary arteriole would display some anti-SLC reactivity (our unpublished observations). Despite high levels of injected labeled mAb, we were unable to detect any SLC on PP-HEVs of DDD/1 mice (Fig. 5).

We reasoned that if T cells relied on SLC triggering of CCR7, and there was substantial variability in PP-HEV presentation of CCR7 ligand SLC, T cell accumulation should colocalize with SLC expression. We observed the behaviors of T cells interacting with PP-HEVs, and then stained these same HEVs in situ for expression of SLC. We found that T cells rolled equally, if not more efficiently, within SLC$^-$ HEV segments, but almost exclusively accumulated on endothelium presenting SLC (Fig. 6 and Fig. 7). Most importantly, T cells rarely accumulated in vessels lacking detectable SLC. In contrast, B cells accumulated without any obvious relationship to SLC expression, occurring in SLC-negative as well as -positive segments (data not shown, but see Fig. 7). These findings not only support the differential requirement for SLC and CCR7 in the triggering of T but not B cell arrest, but suggest that T and B cell arresting factors can be differentially displayed on distinct vascular segments.

Since B cells are recruited into follicles after entry into PPs, we asked whether HEV segments preferentially supporting B cell arrest might be adjacent to or associated with the follicular microenvironments. We coinjected differentially labeled B and T cells and evaluated their accumulation in HEV segments in relation to structural features of the PP. Follicles were identified by the autofluorescence of abundant macrophages within germinal centers, and HEVs could be readily identified at the end of the experiment by injection of labeled mAb to MAdCAM-1 (e.g., see Fig. 5). Although B and T cells could roll in virtually all HEVs, we found a striking segregation of sticking cells: B cells preferentially adhered within segments proximal to or within the periphery of follicles, whereas T cells bound primarily to HEVs within the interfollicular zone (Fig. 8, and see Fig. 7). B cell arrest and accumulation in DDD/1 mice also occur preferentially in follicle-associated HEV segments (data not shown). Our data suggest that lymphoid microenvironmental conditions may regulate HEV display of specialized adhesion-triggering signals that, in turn, may contribute to the selective recruitment of lymphocyte subsets into appropriate follicular versus interfollicular domains.

Discussion

Tissue-selective lymphocyte homing from the blood is controlled by a multistep process involving PTX-sensitive heterotrimeric G protein–linked receptors. These $G_{\alpha i}$-mediated signals trigger integrin-dependent sticking of rolling lymphocytes, and likely participate in their diapedesis and localization within tissue microenvironments. Recently, chemokines have been highlighted as prime candidates that provide PTX-sensitive signals mediating lymphocyte–endothelial recognition and directed migration. Here, we have investigated the role of known rapid adhesion-triggering

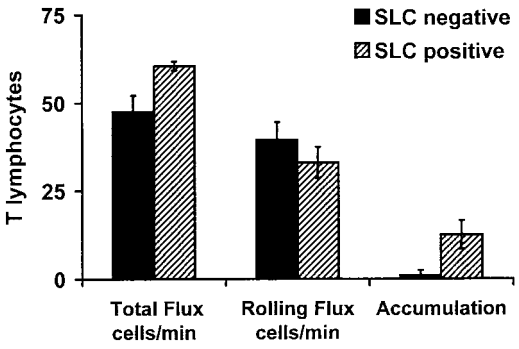

Figure 6. T cells preferentially accumulate in SLC$^+$ HEVs. T cells were observed in HEVs of normal animals as in the legend to Fig. 2. After observations of T cell behaviors in multiple fields, SLC$^+$ HEVs were identified by subsequent, sequential injection of labeled anti-SLC and anti–MAdCAM-1. MAdCAM-1$^+$ HEVs that exhibited successive segments differing only by expression of SLC were analyzed. Data are mean results of three experiments (± SD).

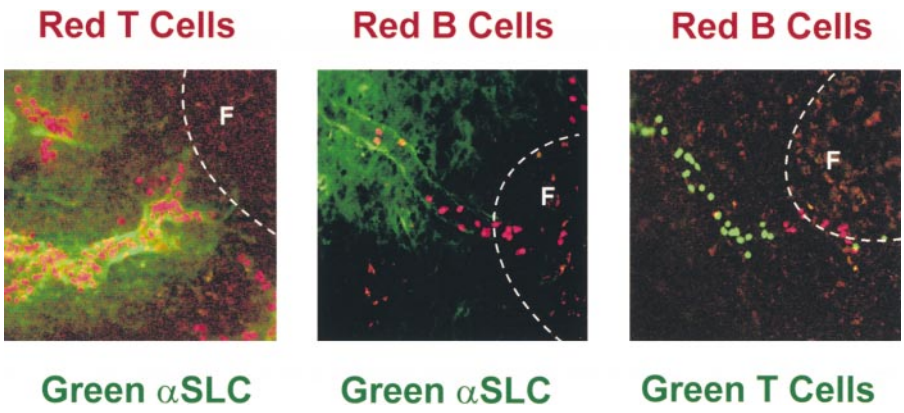

Figure 7. Localization of lymphocytes in PP-HEVs. Micrographs of accumulated lymphocyte subpopulations in PPs. (Left panel) T cells accumulated in SLC^{+} interfollicular segments of HEVs. (Middle panel) B cells in SLC^{low} HEV segments associated with primary follicles. (Right panel) Segregation of sites of preferential T and B cell accumulation in relation to follicles. TRITC-labeled T (left) or B (middle and right panels) cells and CM-FDA-labeled T cells (right panel) were observed in HEVs of normal animals as in the legend to Fig. 4. In the left and middle panels, after lymphocyte accumulation for ~10 min (see Materials and Methods), 60 μg Alexa™ 488–conjugated anti-SLC mAb was injected intravenously to illuminate SLC-expressing HEV segments. Animals were killed, and whole PPs were removed for examination by confocal microscopy. The location of follicles is indicated (F) (20× objective).

chemokines in the recognition of PP-HEVs by circulating B and T lymphocytes. Our data suggest that naive T cells rely upon recognition of luminally presented SLC and use signals mediated by CCR7 to arrest firmly in PP-HEVs. In contrast, B cells, though capable of responding to SLC, use distinct (or additional) mechanisms to arrest in PP-HEVs. Furthermore, we present evidence that differential display of SLC and B cell adhesion-triggering factors by interfollicular versus follicle-associated high endothelium allows microenvironmental control of T versus B cell recruitment from the blood.

With the results presented here, the evidence for CCR7 and SLC involvement in T cell recognition of HEVs seems compelling. Previous studies have shown that HEVs express message for SLC (10), that SLC can trigger rapid integrin-dependent arrest of naive B and T lymphocytes under physiologic shear in vitro (8, 22), and that a selective defect in T cell homing to LNs in DDD/1 mice is associated with deficient SLC and MIP-3β expression (24). Here we show that HEVs in fact display SLC protein, that desensitization of CCR7-mediated signaling with SLC (or MIP-3β) inhibits T cell arrest, and that T cell accumulation correlates with sites of SLC expression. Moreover, we show that the T cell homing deficiency in DDD/1 mice involves a lack of T cell adhesion-triggering responses on HEVs, a phenotype indistinguishable from that of SLC- or MIP-3β–desensitized T cells in wild-type hosts. We conclude that SLC and its receptor CCR7 can mediate T cell recognition of HEVs in lymphoid organs.

These studies provide the first direct evidence of chemokine involvement in adhesion triggering during physiologic lymphocyte–endothelial interactions, thus confirming the hypothesized role of chemokines in lymphocyte–endothelial cell recognition (25). Chemokine-triggered adhesion may be part of a general paradigm in which functionally distinct subsets of circulating lymphocytes use specialized chemokine receptors, in place of or in addition to CCR7, for homing from the blood, especially in settings of inflammation. A significant subset of circulating human memory T cells expresses CCR7 (26; and Campbell, J.J., and L. Wu, unpublished observation), both human and mouse memory T cells respond to SLC and MIP-3β (11, 13, 18, 22, 27, 28), and recent evidence indicates increased expression of CCR7 and concomitant greater response to SLC after activation (13, 14). Thus, memory cells may also use CCR7, like naive T cells, during recirculation through organized lymphoid tissues. Display of other chemokine receptors, such as CXCR3, G protein–coupled receptor GPR-9-6 (CCR9), CCR4, CCR5, and CCR6, also subdivides circulating memory cells, and may help confer unique vascular recognition and tissue- or inflammation-selective homing properties. For example, recent studies suggest a physiological role for CCR4 on systemic memory T cells, and its ligand thymus and activation-regulated chemokine (TARC) displayed by inflamed venules, in the adhesion-triggering step of memory lymphocyte homing to cutaneous sites of inflammation (29), and potentially for CCR9 and its ligand thymus-expressed chemokine (TECK) in intestinal lymphocyte homing (30).

Although our studies implicate SLC receptor(s) in T cell–HEV interactions, and demonstrate SLC presentation by HEV

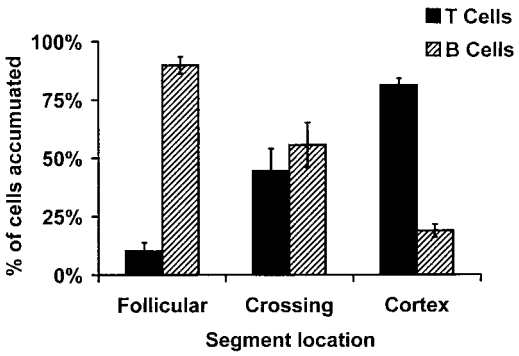

Figure 8. Sticking B and T cells are segregated in PP-HEVs. Accumulated B and T cells in PP-HEVs of normal mice were analyzed for preferential localization after injection of equal numbers of each subset. Follicles were identified by characteristic autofluorescence of resident dendritic cells and macrophages. HEV segments were defined as follicular if lying within or upon a follicle, cortical if wholly within the cortex, and crossing when transitional from follicle to cortex. Red (T) and green (B) accumulated cells were enumerated 8 min after injection in each class of vessels. Data are presented as percentage of B or T cells observed among cells in each vessel type; mean results of three experiments (± SD).

segments mediating T cell accumulation, they do not exclude involvement of MIP-3β (or other unidentified CCR7 ligands) in T cell arrest. Like SLC, MIP-3β has potent chemotactic activity for naive T and B cells, and for subsets of memory CD4 and CD8 cells, but not for granulocytes and monocytes (11, 22, 27, 28). Importantly, MIP-3β acts through the same receptor as SLC, CCR7, can cross-desensitize CCR7 to further signals from either MIP-3β or SLC (22, 31), and, as we have shown here, desensitization with MIP-3β selectively prevents accumulation of T but not B cells in PP-HEVs. MIP-3β is expressed in lymphoid tissues, notably in parafollicular and inner cortical regions of LNs, and by LN stromal elements including dendritic cells derived from T cell zones (11, 32). Although in situ hybridization studies suggest that MIP-3β is not produced by endothelium of HEVs, it is possible that luminal presentation may occur by transcytosis from surrounding tissue. Indeed, findings in other systems demonstrate that chemokines can gain access to the venular lumen even when expressed or introduced in a perivascular location (33). HEV presentation of MIP-3β by this mechanism may account for our inability to block T cell arrest in PP-HEVs with bolus injections of anti-SLC mAbs: intravenous injection of up to 1 mg per mouse yielded only variable and incomplete inhibition of T cell accumulation, never exceeding 50% of control (our unpublished results). However, this may also reflect incomplete blockade of SLC in vivo, as anti-SLC mAbs accumulate only slowly on HEVs (over minutes) compared with anti–MAdCAM-1 mAbs or other anti-endothelial cell antibodies we have used for in situ endothelial visualization. Resolution of the role of MIP-3β or other CCR7 ligands in addition to SLC will require generation of additional, high-affinity anti-SLC and MIP-3β mAbs, and/or evaluation of single and dual gene-targeted mice in future studies.

L-selectin, which is rapidly shed upon cross-linking, has also been shown to transmit signals that can affect integrin affinity (34). Naive B and T lymphocytes interacting with PP-HEVs rely on L-selectin for adequate attachment, and to some degree, for rolling (2, 35). Although chemokine desensitization of T lymphocytes with SLC did not affect attachment and rolling, sticking was abrogated, suggesting that L-selectin signals, if operating in this context, are insufficient to mediate arrest. While we cannot rule out a contribution by L-selectin signaling, particularly for B cells, it is unlikely to be sufficient for physiological adhesion-triggering, given that lymphocyte arrest is PTX sensitive, whereas L-selectin signaling is not (36).

Although we have not here evaluated lymphocyte interactions in situ with LN HEVs, in the course of our studies we noted that some PLN HEVs display SLC, and that desensitization with SLC or MIP-3β prevents accumulation of injected T lymphocytes in LN as well as PP-HEVs. In conjunction with the known deficiency in T cell homing to LNs in DDD/1 mice, these observations suggest that CCR7 and its ligands play comparable roles in T cell adhesion triggering in LNs as in PPs. This postulate has been confirmed in parallel studies from Stein and coworkers (36a).

One of the most interesting discoveries here is the differential vascular interactions of B versus T cells, and their control at the level of adhesion triggering. Accumulation of T and B cell subsets is markedly segregated in PP-HEVs, with T cells collecting preferentially in interfollicular HEV segments, associated with high levels of local SLC expression. Conversely, although B cells can also arrest in SLC^{hi} HEVs, they tend to accumulate within intrafollicular HEV segments, or segments immediately adjacent to follicles—segments which are often $SLC^{low/-}$. This microenvironmental control of T versus B cell interactions with HEVs was surprising in light of earlier models, which assumed that naive B and T cells were recruited equivalently through HEVs, with segregation to their appropriate compartments occurring entirely after entry into the lymphoid tissue parenchyma (37, 38). Indeed, earlier studies of B and T cell interactions with HEVs, using either ex vivo Stamper-Woodruff frozen section assays or short-term homing of adoptively transferred lymphocyte subsets, failed to identify differential association of T versus B cells with HEV segments (39–42; and Butcher, E.C. and I.L. Weissman, unpublished results). This likely reflects the techniques employed, which did not allow visualization of homing interactions, or, in the case of frozen section studies, may not have adequately modeled in vivo physiology. However, these prior studies also focused on HEV interactions in PLNs of young mice, in which follicular domains are characteristically less prominent and less immunologically active than in the PPs studied here. To the extent that the HEV segments recruiting B but not T cells are induced or regulated by the follicular microenvironment, as we propose (see below), it seems likely that such segments would be relatively infrequent and capable of less selective B (versus T) cell recruitment in LNs. It is interesting to note that we have also occasionally observed focal segregation of B and T cell accumulation in MLNs and sheep RBC-immunized PLNs, with B greater than T cell recruitment by subcapsular (follicle-associated) HEVs (data not shown). (In these organs, such segregation is less prominent than in PPs, suggesting that follicular localization might be directed principally by chemotaxis of B cells after extravasation.) Furthermore, consistent with our findings, another study of PPs noted that B cell arrest occurs in a wider range of vessels (by diameter) than T cells, including smaller venules observed inside follicles (43).

In this context, it is noteworthy that early studies of T versus B cell interaction did reveal a relative preference of B versus T cells for PP (versus PLN) HEVs, both in ex vivo frozen section assays and in short-term in vivo homing studies (40, 41). This behavior may be explained in part by the fact that naive B cells display slightly higher levels of the intestinal PP homing receptor α4β7, and slightly lower levels of PLN homing receptor L-selectin, than naive T cells (44, 45). However, it is reasonable to propose that a higher level of B cell adhesion-triggering factors in PP-HEVs (relative to PLN HEVs) could also contribute to their selective localization, as well as to the greater frequency of homed B than T cells in PPs.

The physical structure of the vasculature in PPs may also promote the follicular localization of B cells, as PP-HEVs

first arise from capillary arcades predominantly in or near B cell follicles, and then drain out through parafollicular T cell zones (46). Therefore, the majority of PP-HEVs that cells first encounter lie within the proximal influence of B cell microenvironments, whereas T cell zones effect control over "downstream" HEV segments. Our results show that B cells accumulate efficiently in the upstream, high order, follicle-associated segments in response to an as yet unidentified adhesion-triggering factor(s). In contrast, although T cells efficiently tether and roll in these high order (predominantly SLC^{low} segments in and/or near follicles, they arrest only infrequently. Instead, T cells continue rolling downstream to arrest eventually in lower order SLC^{hi} HEVs located within the interfollicular zone. B cells that escape early recruitment to the follicular segments can also arrest downstream on SLC^{hi} HEVs; whether SLC itself contributes to B cell arrest on these lower order vessels remains to be determined. Thus, the selective homing of T and B cells is determined by their signaling receptors, and not only by disparate levels of counterreceptors for PP-HEV adhesion molecules. Taken together, these studies demonstrate a novel mechanism for the selective recruitment of lymphocyte subsets to specialized lymphoid tissue domains—the differential presentation of factors that trigger firm adhesion.

The segmental control of chemokine expression, as we have demonstrated, is most likely in response to and within the context of microenvironmental cues. PPs and LNs can be extensively remodeled during instances of immune or inflammatory stimulation, and these secondary lymphoid tissues (or their specialized domains) must be capable of rapid and robust architectural refinement, particularly through the specific recruitment of specialized subsets of lymphocytes (47). It will be important to evaluate the extent to which developing lymphoid compartments, or those undergoing acute inflammatory reactions, display altered patterns of chemokine expression on HEVs and within cortical and follicular compartments. Indeed, recent studies of inflamed LNs, PPs, and spleen have demonstrated significant changes in chemokines and adhesion molecules in response to inflammatory challenge, though the relationship to recruitment of lymphocyte subsets has not been examined (48–55; and McEvoy, L.M., unpublished observations). Taken together with our findings, such observations suggest that lymphocyte subset recruitment by LN and PP-HEVs may be tightly controlled through elements of the multistep adhesion cascade, and can be dynamically regulated by altered chemokine display.

In addition to its role in T cell recognition of HEVs, as evidenced here, SLC has been hypothesized to direct migration of lymphocytes and also dendritic cells to and within lymphoid and other tissues (10, 13, 56–58). For example, in situ hybridization and immunohistological studies have revealed high levels of SLC message in the endothelium of lymphatic openings and luminal presentation on lymphatic vessels within extralymphoid tissues, suggesting a potential role of SLC and CCR7 in regulating cellular entry into afferent lymph (10, 59). Consistent with this, recent studies have shown that activated dendritic cells upregulate CCR7, and have provided evidence that SLC is required for efficient dendritic cell recruitment to draining LNs during inflammation (24, 59, 60). It is attractive to postulate that CCR7 and SLC may play a similar role for memory or activated lymphocytes in extravascular recruitment to draining LNs via lymphatics. Furthermore, SLC (as well as MIP-3β) is expressed by stromal cells associated with T cell zones in spleen, thymus, and other lymphoid structures (11, 13, 18, 24, 61, 62). Expression of CCR7 ligands at such sites may serve to recruit or position relevant cells to the appropriate T cell–rich zones, and/or to ensure a close relationship between antigen-presenting stromal cells and naive and antigen-reactive T cells. However, if T cells recruited through SLC^{hi} HEVs are transiently desensitized to SLC, as is possible, regulation of diapedesis and homing into T cell zones would likely require additional chemoattractant mechanisms. If this model is correct, one could imagine that the widespread and high level of expression of CCR7 ligands within T cell zones might serve more to prevent inappropriate "wandering" or retrograde migration of T cells back to HEVs, by establishing a uniform or desensitizing field of CCR7 agonists. Thus, a clear picture of the role of SLC or additional chemotactic factors in extravasation and directed migration of lymphocytes awaits further study.

In conclusion, we have provided direct evidence for chemokine regulation of lymphocyte–endothelial recognition in vivo. Our results indicate that T cell arrest on HEVs can be mediated by SLC and requires signaling through the SLC receptor, CCR7, and demonstrate that B and T cells use distinct adhesion-triggering factors for HEV recognition. Furthermore, we have shown that adhesion-triggering factors for B and T cells are differentially presented in HEV segments, conferring focussed subset recruitment to appropriate, well-defined microenvironments for B and T cell localization within PPs. Thus, our findings demonstrate a fundamental difference in the molecular requirements for T and B cell homing, and reveal a previously unsuspected degree of vascular specialization controlling selective recruitment of circulating lymphocytes, determined not only by tissue type, but also by microdomain.

Consistent with our results, Forster and colleagues (63) have now shown that lymphocytes from CCR7-deficient mice display reduced localization to lymphoid organs, though whether the defect is at the level of HEV interaction or extravasation was not determined. They observed significant reduction of B cell homing as well, especially to LNs: in light of our findings, this may suggest that CCR7 can play a role in B cell diapedesis.

We thank Ms. June Twelves for her excellent technical assistance, Mary Maniscalco for manuscript preparation, and members of our laboratory (especially Eddie Bowman, Eric Kunkel, and Uwe Gosslar), as well as Jens Stein and Ulrich von Andrian for helpful discussions of ongoing work.

This work was supported by National Institutes of Health grants GM37734 and AI37832, by National Institutes of Health Training Grant 5T32 AI07290 (to R.A.Warnock), and by a Postdoctoral Fellowship from the Arthritis Foundation (to J.J. Campbell).

Submitted: 9 June 1999
Revised: 8 September 1999
Accepted: 12 October 1999

Note added in proof. Vassileva et al. have now shown that there are two SLC genes in mice, and that the DDD/1 (*plt*) mouse mutation is a deletion of the gene responsible for SLC expression in lymphoid tissues (Vassileva, G., H. Soto, A. Zlotnik, H. Nakano, T. Kakiuchi, J.A. Hedrick, and S.A. Lira. 1999. *J. Exp. Med.* 190: 1183–1188).

References

1. Bargatze, R.F., and E.C. Butcher. 1993. Rapid G protein–regulated activation event involved in lymphocyte binding to high endothelial venules. *J. Exp. Med.* 178:367–372.
2. Bargatze, R.F., M.A. Jutila, and E.C. Butcher. 1995. Distinct roles of L-selectin and integrins alpha 4 beta 7 and LFA-1 in lymphocyte homing to Peyer's patch-HEV in situ: the multistep model confirmed and refined. *Immunity*. 3:99–108.
3. Warnock, R.A., S. Askari, E.C. Butcher, and U.H. von Andrian. 1998. Molecular mechanisms of lymphocyte homing to peripheral lymph nodes. *J. Exp. Med.* 187:205–216.
4. Butcher, E.C., M. Williams, K. Youngman, L. Rott, and M. Briskin. 1999. Lymphocyte trafficking and regional immunity. *Adv. Immunol.* 72:209–253.
5. Salmi, M., S. Tohka, E.L. Berg, E.C. Butcher, and S. Jalkanen. 1997. Vascular adhesion protein 1 (VAP-1) mediates lymphocyte subtype–specific, selectin-independent recognition of vascular endothelium in human lymph nodes. *J. Exp. Med.* 186:589–600.
6. Kim, C.H., and H.E. Broxmeyer. 1999. Chemokines: signal lamps for trafficking of T and B cells for development and effector function. *J. Leukoc. Biol.* 65:6–15.
7. Zlotnik, A., J. Morales, and J.A. Hedrick. 1999. Recent advances in chemokines and chemokine receptors. *Crit. Rev. Immunol.* 19:1–47.
8. Campbell, J.J., J. Hedrick, A. Zlotnik, M.A. Siani, D.A. Thompson, and E.C. Butcher. 1998. Chemokines and the arrest of lymphocytes rolling under flow conditions. *Science*. 279:381–384.
9. Bleul, C.C., R.C. Fuhlbrigge, J.M. Casasnovas, A. Aiuti, and T.A. Springer. 1996. A highly efficacious lymphocyte chemoattractant, stromal cell–derived factor 1 (SDF-1). *J. Exp. Med.* 184:1101–1109.
10. Gunn, M.D., K. Tangemann, C. Tam, J.G. Cyster, S.D. Rosen, and L.T. Williams. 1998. A chemokine expressed in lymphoid high endothelial venules promotes the adhesion and chemotaxis of naive T lymphocytes. *Proc. Natl. Acad. Sci. USA*. 95:258–263.
11. Ngo, V.N., H.L. Tang, and J.G. Cyster. 1998. Epstein-Barr virus–induced molecule 1 ligand chemokine is expressed by dendritic cells in lymphoid tissues and strongly attracts naive T cells and activated B cells. *J. Exp. Med.* 188:181–191.
12. Williams, M.B., and E.C. Butcher. 1997. Homing of naive and memory T lymphocyte subsets to Peyer's patches, lymph nodes, and spleen. *J. Immunol.* 159:1746–1752.
13. Willimann, K., D.F. Legler, M. Loetscher, R.S. Roos, M.B. Delgado, I. Clark-Lewis, M. Baggiolini, and B. Moser. 1998. The chemokine SLC is expressed in T cell areas of lymph nodes and mucosal lymphoid tissues and attracts activated T cells via CCR7. *Eur. J. Immunol.* 28:2025–2034.
14. Nagira, M., T. Imai, R. Yoshida, S. Takagi, M. Iwasaki, M. Baba, Y. Tabira, J. Akagi, H. Nomiyama, and O. Yoshie. 1998. A lymphocyte-specific CC chemokine, secondary lymphoid tissue chemokine (SLC), is a highly efficient chemoattractant for B cells and activated T cells. *Eur. J. Immunol.* 28: 1516–1523.
15. Pachynski, R.K., S.W. Wu, M.D. Gunn, and D.J. Erle. 1998. Secondary lymphoid-tissue chemokine (SLC) stimulates integrin alpha 4 beta 7-mediated adhesion of lymphocytes to mucosal addressin cell adhesion molecule-1 (MAdCAM-1) under flow. *J. Immunol.* 161:952–956.
16. Gallatin, W.M., I.L. Weissman, and E.C. Butcher. 1983. A cell-surface molecule involved in organ-specific homing of lymphocytes. *Nature*. 304:30–34.
17. Streeter, P.R., E.L. Berg, B.T. Rouse, R.F. Bargatze, and E.C. Butcher. 1988. A tissue-specific endothelial cell molecule involved in lymphocyte homing. *Nature*. 331:41–46.
18. Tanabe, S., Z. Lu, Y. Luo, E.J. Quackenbush, M.A. Berman, L.A. Collins-Racie, S. Mi, C. Reilly, D. Lo, K.A. Jacobs, and M.E. Dorf. 1997. Identification of a new mouse beta-chemokine, thymus-derived chemotactic agent 4, with activity on T lymphocytes and mesangial cells. *J. Immunol.* 159: 5671–5679.
19. Sanchez-Madrid, F., P. Simon, S. Thompson, and T.A. Springer. 1983. Mapping of antigenic and functional epitopes on the alpha- and beta-subunits of two related mouse glycoproteins involved in cell interactions, LFA-1 and Mac-1. *J. Exp. Med.* 158:586–602.
20. Bohm, S.K., E.F. Grady, and N.W. Bunnett. 1997. Regulatory mechanisms that modulate signalling by G-protein-coupled receptors. *Biochem. J.* 322:1–18.
21. Ye, R.D., and F. Boulay. 1997. Structure and function of leukocyte chemoattractant receptors. *Adv. Pharmacol.* 39: 221–289.
22. Campbell, J.J., E.P. Bowman, K. Murphy, K.R. Youngman, M.A. Siani, D.A. Thompson, L. Wu, A. Zlotnik, and E.C. Butcher. 1998. 6-C-kine (SLC), a lymphocyte adhesion-triggering chemokine expressed by high endothelium, is an agonist for the MIP-3β receptor CCR7. *J. Cell Biol.* 141:1053–1059.
23. Nakano, H., T. Tamura, T. Yoshimoto, H. Yagita, M. Miyasaka, E.C. Butcher, H. Nariuchi, T. Kakiuchi, and A. Matsuzawa. 1997. Genetic defect in T lymphocyte-specific homing into peripheral lymph nodes. *Eur. J. Immunol.* 27:215–221.
24. Gunn, M.D., S. Kyuwa, C. Tam, T. Kakiuchi, A. Matsuzawa, L.T. Williams, and H. Nakano. 1999. Mice lacking expression of secondary lymphoid organ chemokine have defects in lymphocyte homing and dendritic cell localization. *J. Exp. Med.* 189:451–460.
25. Butcher, E.C. 1991. Leukocyte-endothelial cell recognition: three (or more) steps to specificity and diversity. *Cell*. 67: 1033–1036.
26. Sallusto, F., D. Lenig, R. Forster, M. Lipp, and A. Lanzavecchia. 1999. Two subsets of memory T lymphocytes with distinct homing potentials and effector functions. *Nature*. 401: 708–712.
27. Kim, C.H., L.M. Pelus, J.R. White, E. Applebaum, K. Johanson, and H.E. Broxmeyer. 1998. CK beta-11/macrophage inflammatory protein-3 beta/EBI1-ligand chemokine is an efficacious chemoattractant for T and B cells. *J. Immunol.* 160:2418–2424.
28. Yoshida, R., M. Nagira, T. Imai, M. Baba, S. Takagi, Y. Tabira, J. Akagi, H. Nomiyama, and O. Yoshie. 1998. EBI1-ligand chemokine (ELC) attracts a broad spectrum of lymphocytes: activated T cells strongly up-regulate CCR7 and

efficiently migrate toward ELC. *Int. Immunol.* 10:901–910.
29. Campbell, J.J., G. Haraldsen, J. Pan, J. Rottman, S. Qin, P. Ponath, D.P. Andrew, R. Warnke, N. Ruffing, N. Kassam, et al. 1999. The chemokine receptor CCR4 in vascular recognition by cutaneous but not intestinal memory T cells. *Nature*. 400:776–780.
30. Zabel, B.A., W.W. Agace, J.J. Campbell, H.M. Heath, D. Parent, A.I. Roberts, E.C. Ebert, N. Kassam, S. Qin, M. Zovko, et al. 1999. Human G protein–coupled receptor GPR-9-6/CC chemokine receptor 9 is selectively expressed on intestinal homing T lymphocytes, mucosal lymphocytes, and thymocytes and is required for thymus-expressed chemokine–mediated chemotaxis. *J. Exp. Med.* 190:1241–1256.
31. Yoshida, R., M. Nagira, M. Kitaura, N. Imagawa, T. Imai, and O. Yoshie. 1998. Secondary lymphoid-tissue chemokine is a functional ligand for the CC chemokine receptor CCR7. *J. Biol. Chem.* 273:7118–7122.
32. Yoshida, R., T. Imai, K. Hieshima, J. Kusuda, M. Baba, M. Kitaura, M. Nishimura, M. Kakizaki, H. Nomiyama, and O. Yoshie. 1997. Molecular cloning of a novel human CC chemokine EBI1-ligand chemokine that is a specific functional ligand for EBI1, CCR7. *J. Biol. Chem.* 272:13803–13809.
33. Middleton, J., S. Neil, J. Wintle, I. Clark-Lewis, H. Moore, C. Lam, M. Auer, E. Hub, and A. Rot. 1997. Transcytosis and surface presentation of IL-8 by venular endothelial cells. *Cell.* 91:385–395.
34. Gopalan, P.K., C.W. Smith, H. Lu, E.L. Berg, L.V. McIntire, and S.I. Simon. 1997. Neutrophil CD18-dependent arrest on intercellular adhesion molecule 1 (ICAM-1) in shear flow can be activated through L-selectin. *J. Immunol.* 158: 367–375.
35. Kunkel, E.J., C.L. Ramos, D.A. Steeber, W. Muller, N. Wagner, T.F. Tedder, and K. Ley. 1998. The roles of L-selectin, beta 7 integrins, and P-selectin in leukocyte rolling and adhesion in high endothelial venules of Peyer's patches. *J. Immunol.* 161:2449–2456.
36. Laudanna, C., G. Constantin, P. Baron, E. Scarpini, G. Scarlato, G. Cabrini, C. Dechecchi, F. Rossi, M.A. Cassatella, and G. Berton. 1994. Sulfatides trigger increase of cytosolic free calcium and enhanced expression of tumor necrosis factor-alpha and interleukin-8 mRNA in human neutrophils. Evidence for a role of L-selectin as a signaling molecule. *J. Biol. Chem.* 269:4021–4026.
36a. Stein, J.V., A. Rot, Y. Luo, M. Narasimhaswamy, H. Nakano, M.D. Gunn, A. Matsuzawa, E.J. Quackenbush, M.E. Dorf, and U.H. von Andrian. 2000. The CC chemokine thymus-derived chemotactic agent 4 (TAC-4, secondary lymphoid tissue chemokine 6Ckine, Exodus-2) triggers lymphocyte function–associated antigen 1–arrest of rolling T lymphocytes in peripheral node high endothelial venules. *J. Exp. Med.* 191: 61–75.
37. Weissman, I.L., G.A. Gutman, and S.H. Friedberg. 1974. Tissue localization of lymphoid cells. *Ser. Haematol.* 7:482–504.
38. Goodnow, C.C., and J.G. Cyster. 1997. Lymphocyte homing: the scent of a follicle. *Curr. Biol.* 7:R219–R222.
39. Gutman, G.A., and I.L. Weissman. 1973. Homing properties of thymus-independent follicular lymphocytes. *Transplantation*. 16:621–629.
40. Stevens, S.K., I.L. Weissman, and E.C. Butcher. 1982. Differences in the migration of B and T lymphocytes: organ-selective localization in vivo and the role of lymphocyte-endothelial cell recognition. *J. Immunol.* 128:844–851.
41. Pals, S.T., G. Kraal, E. Horst, A. de Groot, R.J. Scheper, and C.J. Meijer. 1986. Human lymphocyte-high endothelial venule interaction: organ-selective binding of T and B lymphocyte populations to high endothelium. *J. Immunol.* 137: 760–763.
42. Pellas, T.C., and L. Weiss. 1990. Migration pathways of recirculating murine B cells and CD4+ and CD8+ T lymphocytes. *Am. J. Anat.* 187:355–373.
43. Miura, S., Y. Tsuzuki, D. Fukumura, H. Serizawa, M. Suematsu, I. Kurose, H. Imaeda, H. Kimura, H. Nagata, M. Tsuchiya, et al. 1995. Intravital demonstration of sequential migration process of lymphocyte subpopulations in rat Peyer's patches. *Gastroenterology*. 109:1113–1123.
44. Andrew, D.P., L.S. Rott, P.J. Kilshaw, and E.C. Butcher. 1996. Distribution of alpha 4 beta 7 and alpha E beta 7 integrins on thymocytes, intestinal epithelial lymphocytes and peripheral lymphocytes. *Eur. J. Immunol.* 26:897–905.
45. Tang, M.L., D.A. Steeber, X.Q. Zhang, and T.F. Tedder. 1998. Intrinsic differences in L-selectin expression levels affect T and B lymphocyte subset-specific recirculation pathways. *J. Immunol.* 160:5113–5121.
46. Yamaguchi, K., and G.I. Schoefl. 1983. Blood vessels of the Peyer's patch in the mouse: I. Topographic studies. *Anat. Rec.* 206:391–401.
47. Butcher, E.C., and L.J. Picker. 1996. Lymphocyte homing and homeostasis. *Science*. 272:60–66.
48. Mebius, R.E., J. Breve, A.M. Duijvestijn, and G. Kraal. 1990. The function of high endothelial venules in mouse lymph nodes stimulated by oxazolone. *Immunology.* 71:423–427.
49. van Halteren, A.G., R.E. Mebius, and G. Kraal. 1994. Vascular addressin expression in Peyer's patches: an in vivo study of site-associated regulation. *Adv. Exp. Med. Biol.* 355:125–130.
50. Mebius, R.E., P.R. Streeter, S. Michie, E.C. Butcher, and I.L. Weissman. 1996. A developmental switch in lymphocyte homing receptor and endothelial vascular addressin expression regulates lymphocyte homing and permits CD4+ CD3− cells to colonize lymph nodes. *Proc. Natl. Acad. Sci. USA*. 93:11019–11024.
51. Kraal, G., and R.E. Mebius. 1997. High endothelial venules: lymphocyte traffic control and controlled traffic. *Adv. Immunol.* 65:347–395.
52. Cuff, C.A., J. Schwartz, C.M. Bergman, K.S. Russell, J.R. Bender, and N.H. Ruddle. 1998. Lymphotoxin alpha3 induces chemokines and adhesion molecules: insight into the role of LT alpha in inflammation and lymphoid organ development. *J. Immunol.* 161:6853–6860.
53. Connor, E.M., M.J. Eppihimer, Z. Morise, D.N. Granger, and M.B. Grisham. 1999. Expression of mucosal addressin cell adhesion molecule-1 (MAdCAM-1) in acute and chronic inflammation. *J. Leukoc. Biol.* 65:349–355.
54. Ngo, V.N., H. Korner, M.D. Gunn, K.N. Schmidt, D.S. Riminton, M.D. Cooper, J.L. Browning, J.D. Sedgwick, and J.G. Cyster. 1999. Lymphotoxin α/β and tumor necrosis factor are required for stromal cell expression of homing chemokines in B and T cell areas of the spleen. *J. Exp. Med.* 189:403–412.
55. Tanaka, Y., T. Imai, M. Baba, I. Ishikawa, M. Uehira, H. Nomiyama, and O. Yoshie. 1999. Selective expression of liver and activation-regulated chemokine (LARC) in intestinal epithelium in mice and humans. *Eur. J. Immunol.* 29:633–642.
56. Sozzani, S., P. Allavena, G. D'Amico, W. Luini, G. Bianchi, M. Kataura, T. Imai, O. Yoshie, R. Bonecchi, and A. Mantovani. 1998. Differential regulation of chemokine receptors during dendritic cell maturation: a model for their trafficking

properties. *J. Immunol.* 161:1083–1086.
57. Sallusto, F., P. Schaerli, P. Loetscher, C. Schaniel, D. Lenig, C.R. Mackay, S. Qin, and A. Lanzavecchia. 1998. Rapid and coordinated switch in chemokine receptor expression during dendritic cell maturation. *Eur. J. Immunol.* 28:2760–2769.
58. Yanagihara, S., E. Komura, J. Nagafune, H. Watarai, and Y. Yamaguchi. 1998. EBI1/CCR7 is a new member of dendritic cell chemokine receptor that is up-regulated upon maturation. *J. Immunol.* 161:3096–3102.
59. Saeki, H., A.M. Moore, M.J. Brown, and S.T. Hwang. 1999. Cutting edge: secondary lymphoid-tissue chemokine (SLC) and CC chemokine receptor 7 (CCR7) participate in the emigration pathway of mature dendritic cells from the skin to regional lymph nodes. *J. Immunol.* 162:2472–2475.
60. Kellermann, S.A., S. Hudak, E.R. Oldham, Y.J. Liu, and L.M. McEvoy. 1999. The CC chemokine receptor-7 ligands 6Ckine and macrophage inflammatory protein-3beta are potent chemoattractants for in vitro- and in vivo-derived dendritic cells. *J. Immunol.* 162:3859–3864.
61. Nagira, M., T. Imai, K. Hieshima, J. Kusuda, M. Ridanpaa, S. Takagi, M. Nishimura, M. Kakizaki, H. Nomiyama, and O. Yoshie. 1997. Molecular cloning of a novel human CC chemokine secondary lymphoid-tissue chemokine that is a potent chemoattractant for lymphocytes and mapped to chromosome 9p13. *J. Biol. Chem.* 272:19518–19524.
62. Hedrick, J.A., and A. Zlotnik. 1997. Identification and characterization of a novel beta chemokine containing six conserved cysteines. *J. Immunol.* 159:1589–1593.
63. Forster, R., A. Schubel, D. Breitfeld, E. Kremmer, I. Renner-Muller, E. Wolf, and M. Lipp. 1999. CCR7 coordinates the primary immune response by establishing functional microenvironments in secondary lymphoid organs. *Cell.* 99:23–33.